MODELLING SUMMER WATER TEMPERATURE ON THE YENISEI RIVER

by

Nikolay Y. SHAPAREV[a,b*]

[a]Institute of Computational Modelling of the Siberian Branch of the Russian Academy of Science, Krasnoyarsk, Russia
[b]Siberian Federal University, Krasnoyarsk, Russia

Original scientific paper
https://doi.org/10.2298/TSCI19S2607S

A summertime hydrothermal regime of the Yenisei River downstream of the Krasnoyarsk hydroelectric power plant is modeled based on a deterministic approach. To that end, the Fourier equation is used and the following physical processes contributing to the heat exchange between water and the surroundings are taken into consideration: absorption of direct and scattered solar radiation by water, absorption of downwelling thermal infrared radiation from the atmosphere by water surface, thermal infrared radiation back from the water surface, convection of heat and heat loss due to evaporation of water. A clear-skies river thermal regime under no wind is studied in a 124-km stream reach below the power plant and the obtained results are compared against temperatures recorded at gauging stations.

Key words: *water temperature, the Yenisei River, modelling*

Introduction

The Yenisei River in terms of runoff is the largest in Russia (599 km^3/year) and seventh largest in world (1.5% of global runoff) [1]. There are six hydroelectric power plants (HPP) built in the basin of the river. One of them – Krasnoyarsk HPP is among the top ten world's most powerful HPP (6000 MW) and is the key anthropogenic factor influencing the Yenisei River. Upstream, above the dam, a reservoir of 73 km^3 capacity has been built. Water from the bottom strata of this reservoir flows through the dam and enters the afterbay of the Krasnoyarsk HPP. The incoming water temperature over year varies between 2 ^oC and 12 ^oC. As a result, downstream of the HPP summer water temperatures are lower and winter temperatures are higher than these before the stream has been regulated. Temperature is an important parameter as it influences the behavior of hydrophysical, hydrochemical, and hydrobiological processes.

Here we consider the summertime hydrothermal regime in a 124-km river reach downstream of the Krasnoyarsk HPP on July 3, 2016 based on the deterministic modelling approach. The physical heat exchange processes include absorption of direct and scattered solar radiation by water, absorption of downwelling thermal infrared radiation (TIR) from the atmosphere by the water surface, TIR back from the water surface, convection of heat and

* Author's e-mail: shaparev@icm.krasn.ru

heat loss due to evaporation of water. To carry out mathematical simulation by analogy with other authors [2-6], we use the Fourier equation. Next we switch to a co-ordinate system moving with water and end up with a simple differential equation for water temperature. With this equation we can predict longitudinal water temperature fluctuation along the river at various times considering real morphometric characteristics. The water temperatures obtained by modelling are compared against the observed temperatures recorded at the gauging stations and thereby adequacy of the applied physical-mathematical models to the real hydrothermal processes is assessed.

Mathematical and physical modelling of the hydrothermal regime

Water from the upstream reservoir is released through the dam and enters the afterbay of surface width, B [m], and cross-sectional area, S [m^2]. Water discharge through the dam body is characterized by the quantity, Q [m^{3}sec^{-1}]. The mean streamflow velocity, V [km hr^{-1}], is:

$$V = \frac{Q}{S} \tag{1}$$

The hydrothermal river regime in this situation can be described by the Fourier equation:

$$\frac{\partial T_w(x,t)}{\partial t} = -V(x)\frac{\partial T_w(x,t)}{\partial x} + D\frac{\partial^2 T_w(x,t)}{\partial x^2} + \frac{W(t)}{\rho c}\frac{B(x)}{S(x)} \tag{2}$$

where T_w [^{o}C] is the cross-sectional average water temperature, t [hour] – the time, x [km] – the distance downstream of dam, D [m^{2}sec^{-1}] – the dispersion coefficient in the direction of flow, ρ [1000 kgm^{-3}] – the specific water density, c [4.19·10^{-3} J kg^{-1o}C^{-1}] – the specific heat of water, and W [Wm^{-2}] – the heat transfer power between water and the surroundings which equals:

$$W(t) = W_s + W_a - W_w + W_c - W_e \tag{3}$$

where W_s the direct and scattered down welling solar radiation absorbed by water, W_a – the atmospheric TIR absorbed by water, W_w – the TIR from water surface to the atmosphere, W_c – the convective heat transfer from water to the atmosphere, and W_e is the loss of heat due to evaporation.

Hence with a typical flow velocity of 2 [m/sec] in the downstream reach, the thermal conductivity can be neglected. Then in the system of co-ordinates moving at a velocity $V(x)$. Equation (2) is rewritten:

$$\frac{\mathrm{d}T_w(t)}{\mathrm{d}t} = \frac{W(t)}{\rho c}\frac{B[x(t)]}{S[x(t)]} \tag{4}$$

solution of which is found from the expression:

$$T_w(t) = \frac{1}{\rho c}\int_{t_0}^{t}\frac{B[x(t)]}{S[x(t)]}W(t)\mathrm{d}t + T_w(0,t_0), \quad x(t) = Q\int_{t_0}^{t}\frac{\mathrm{d}t}{S[x(t)]} \tag{5}$$

where $T_w(0,t_0)$ is the outflow temperature of water leaving the dam at time, t_0.

The power of extraterrestrial solar radiation equals [7]:

$$F = F_0 E \cos\theta, \quad \cos\theta = \sin\varphi \cdot \sin\delta + \cos\varphi \cdot \cos\delta \cdot \cos\omega t' \tag{6}$$

where F_0 = 1367 Wm^{-2} is the solar constant, E – the eccentricity correction factor, θ – the zenith angle, t' – time from noon, ω – the rotational speed of the Earth around its polar axis, and φ = 55.94º is the geographic latitude of the HPP location. The solar declination on July 3, 2016 was δ = 22.97º and E = 0.966. Note that diurnal variation of δ was insignificant therefore the sunrise and sunset times are both determined by the condition F = 0. From eq. (6) we then have:

$$\cos\omega t' = -\mathrm{tg}\varphi\ \mathrm{tg}\delta \tag{7}$$

Consequently, the negative root of the expression, $-\omega t'$, refers to the sunrise and the positive one, $\omega t'$, to the sunset. Since t' is the time from noon, we further have:

$$\cos\omega t' = \cos\left(\pi\frac{t - t_n}{12}\right) \tag{8}$$

where t_n is the time of solar noon and t is time from midnight. From eq. (7) we have t_{sr} = 4.06 hours for the sunrise and t_{ss} = 21.57 hours for the sunset. Then the length of day is 15.51 hours and the time of noon will be t_n = 12.81 hours. Temporal behavior of the power of extraterrestrial solar radiation is described by eq. (6) and is shown in fig. 1 (curve 1).

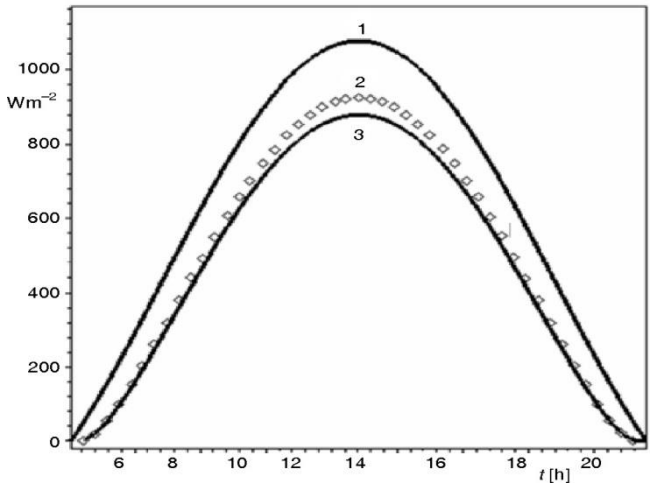

Figure 1. Temporal dependence of the solar radiation power;
1 – incident on the Earth's atmosphere, 2 – transferred through the atmosphere, 3 – absorbed by water

According to the Bouguer-Lambert-Beer law, the power of solar radiation reaching the water surface is:

$$F' = F\exp\left(-\frac{\tau_0}{\cos\theta}\right) \tag{9}$$

where optical thickness of the atmosphere which taking into account the scattered radiation is $\tau_0 \simeq 0.12$ [6]. The power of direct and scattered solar radiation incident on water surface is found from expression (9) and is shown in fig. 1 (curve 2).

Upon reaching a plane water surface, solar radiation is partially reflected. The reflection coefficient, R, is calculated by the Fresnel's formula:

$$W_s = (1-R)F' \tag{10}$$

The power of solar radiation absorbed by water is shown in fig. 1 (curve 3). Temporal dependence of solar energy absorbed by water is obtained by integrating expression (10) over time and is given in fig. 2.

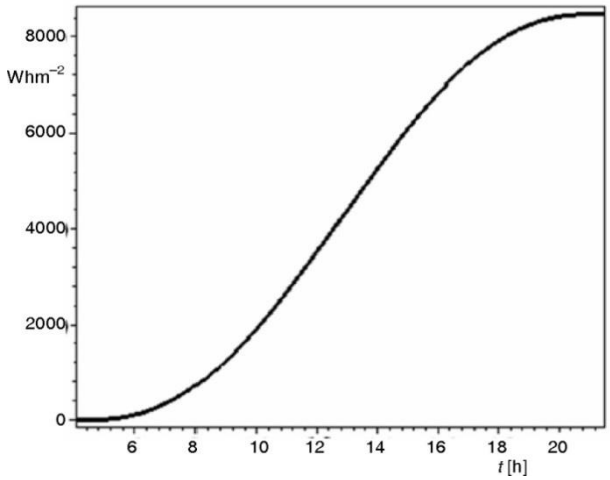

Figure 2. Temporal dependence of solar energy absorbed by water

Water surface emits TIR defined by the Stefan-Boltzmann law:

$$W_w = \varepsilon_w \sigma (273+T_w)^4 \tag{11}$$

where ε_w is emissivity of the water surface, which is ε_w = 0.995 according to [8]. The Stefan-Boltzmann constant is $\sigma = 5.67 \cdot 10^{-8}$ (Wm^{-2}K^{-4}). For T_w = 7.2 ºC we have W_w = 290 Wm^{-2}. While emitting this energy the water gets colder.

Over years, various empirical formulas have been proposed to calculate the atmospheric emission coefficient, ε_a. An overview of these is given in [9]. Our analysis has shown that the best suited formula for our situation is the one proposed by [10] because the optical thickness of the atmosphere in the wavelength range 9.8 μm is close to unity [11]:

$$\varepsilon_a = 1 - 0.4 \exp\left(-\frac{100 e_a}{T_a + 273}\right) \tag{12}$$

where T_a [°C] is the temperature of the atmosphere and e_a [mb] is the atmospheric water vapor pressure equal to:

$$e_a = \frac{H}{100} e_s \tag{13}$$

where e_s [mb] is the saturation vapor pressure estimated from:

$$e_s = 6.1 \exp\left(\frac{17.27 \cdot T_a}{273 + T_a}\right) \tag{14}$$

where H is the atmospheric humidity. We now can carry out calculations for July 3, 2016. At noon T_a = 26 ºC and the humidity was H = 45%, at midnight T_a = 14 ºC, H = 85%. Then we have ε_a = 0.99, W_a = 460 Wm^{-2} at noon and ε_a = 0.99, W_a = 390 Wm^{-2} at midnight. Atmospheric TIR is absorbed by water surface and increases the water temperature.

The energy spent on water evaporation W_e, is estimated as [12-14]:

$$W_e = \rho L\, f(w)(e_s - e_a) \tag{15}$$

where $L = 2.26 \cdot 10^6$ Jkg^{-1} is the latent heat of evaporation. When the wind velocity is w = 0, we have $f \simeq 3 \cdot 10^{-9}$ (mb^{-1}ms^{-1}) according to the data from [15]. For the quoted data we have W_e = 31 Wm^{-2} at noon and W_e = 4.6 Wm^{-2} at midnight, which results in the drop of the water temperature.

Convective heat flux is estimated as [16]:

$$W_c = 0.61 \rho L\, f(T_w - T_a) \tag{16}$$

Thus, convective heating is 25 Wm^{-2} at noon and 1.3 Wm^{-2} at midnight. The difference between evaporation and convection is 6 Wm^{-2} during the daytime and 3.3 Wm^{-2} at night. So, the heat budget is dominated by evaporation and the water gets colder.

Spatial-temporal distribution of water temperature along the river course

We consider a 124-km reach of the Yenisei River downstream the dam of the Krasnoyarsk HPP. The reach is divided by 4 cross-section lines at (0.5, 40, 77, 124 km) with gauging stations at the first, second and forth section lines to measure water temperature. The first station is located next to the dam (x = 0.5 km) and measures water temperature leaving the dam. The other two are located at 40 km and 124 km downstream. Streamflow velocity is assumed constant from section to section and is found from eq. (1) at Q = 2900 m^{3}sec^{-1}. The S is equal to the cross-sectional area of the downstream lowest reach section. Flow time between section lines is found as the section-to-section distance divided by the flow velocity. Temperature measurements at the gauging stations are taken at time, t_g (at 8.00 and 20.00 hour). Water leaves the dam at time $t_0 = t_g - t_i$ where t_i is the length of time within which water from the dam reaches a cross-section line. Water temperature was computed using eq. (5) which now has the form:

$$T_W(t) = \frac{1}{\rho c} \sum_{i=2}^{4} \frac{B_i[x_i(t)]}{S_i[x_i(t)]} \quad W_i \Delta t_i + T_W(0, t_0), \quad \Delta t_1 = t_i - t_{i-1} \tag{17}$$

where i is the reach section number, Δt_i – the flow time between the $i - 1$ and i section lines, $W_i \Delta t_i$ – the energy received by water along each reach section. Power W_i depends on day or night time, water and atmospheric temperature, water vapor pressure, and humidity. The amount of solar power absorbed by water over time between $t_{i-1}$and t_i was found from fig. 2. The power emitted by water is 290 Wm^{-2}. The atmospheric radiation power was assumed 460 Wm^{-2} at daytime and 390 Wm^{-2} at night. The difference in power between evaporation and convection is 6 Wm^{-2} during the daytime and 3.3 Wm^{-2} during the nighttime. Water temperature at the first gauging station was $T_w(0, t_0) = 7.2$ °C and remained constant during the time period under consideration. Morphometric and hydrophysical characteristics of the river reach sections are summarized in tab. 1.

Table 1. Morphometric and hydrophysical characteristics

Cross-section line number		1	2	3	4
Dam-to-section line distance, [km]		0.5	40	77	124
Width B, [m]		520	830	580	450
Cross-sectional area S, [m^2]		1834	2254	2452	2513
Stream flow velocity, [km/hour]		5.7	4.6	4.3	3.7
Flow time between adjacent cross-section lines, Δt_i, [hours]			7.6	9.5	11.9
Relation B/S, [m^{-1}]		0.283	0.368	0.236	0.179
T_w July 3 at 8.00, ºC	Calculated		7.7	8.7	10.1
	Measured	7.2	8.0		10
T_w July 3 at 20.00, ºC	Calculated		9.0	9.9	10.3
	Measured	7.2	9.0		10.6

Let us calculate water temperature at the second section line at 8.00 on July 3, 2016. Water leaves the dam at 0.4 and in 7.6 hours reaches the second gauging station at 8.00. The energy difference between atmospheric radiation and emission from water will be 400 Whm^{-2} at night and 617 Whm^{-2} during the daytime. The amount of solar energy absorbed by 8.00 is 716 Whm^{-2}. The rate of water energy drop due to evaporation and convection was 13.2 Whm^{-2} at night and 21.6 Whm^{-2} at daytime. The total net energy received by water by 8.00 will be 1695 Whm^{-2}. Then, for B/S = 0.368, according to eq. (14), water temperature at the second section line at 8.00 will be 7.7 ^{o}C. The observed water temperature recorded at the station was 8 ^{o}C. When temperature measurements at the second gauging station are taken at 20.00, water leaves the dam at 12.4. The difference between atmospheric radiation and water emission will be 1292 Whm^{-2}. Solar energy over the time period from 12.4 to 20.00 amounts to 4463 Whm^{-2}. The energy loss caused by evaporation and convection will be 45.6 Whm^{-2}. The net energy received by water will total at 5709 Whm^{-2} and the water temperature will be 9 ^{o}C. The actual temperature recorded at the second station was T_w = 9 ºC.

Next we calculate water temperature at the third section line on July 3, 2016 at 8.00. Water leaves the dam at 14.9 on July 2 and in 17.1 hours arrives at the third section next day at 8.00. By the second gauging station, the atmospheric radiation energy less emission from water is 1222 Whm^{-2}, solar energy is 2392 Whm^{-2}, and the energy of convective and evaporative processes is 76.6 Whm^{-2}. Upon reaching the second section line the water temperature changes as much as ΔT_w = 1.1 ºC. Between the second and third sections, water receives energy at the rate of 1913 Whm^{-2} and the water temperature will increase by 0.4 ^{o}C. Then the water temperature at the third section line at 8.00 will be T_w = 8.7 ºC. Water leaving the dam at hour 2.9 on July 3 enters the third reach section at 20.00. While traveling to the second station, water gains 1222 Whm^{-2} due to TIR absorption and 2280 Whm^{-2} due to solar radiation flux and loses energy at a rate of 25 Whm^{-2} because of convective and evaporative processes. The water temperature upon reaching the second station will change by ΔT_w = 1.1 ºC. The energy gained by water between the second and third section lines will be 7812 Whm^{-2} and the temperature will increase by ΔT_w = 1.6 ºC. Hence the calculated temperature at the third section line at 20.00 will be T_w = 9.9 ºC.

Water leaving the dam at hour 3.00 on July, 2 will reach the fourth section line at 8.00 on July, 3. When water arrives at the second gauging station its energy will have increased as much as 3431 Whm^{-2} and the temperature changed by ΔT_w = 1.1 ºC. The water

energy increase at the third section line will be 7655 Whm^{-2} and the water temperature will change by ΔT_w = 1.5 ºC. Finally, upon reaching the fourth section line the energy gain will be as much as 2259 Whm^{-2} and the temperature will change by ΔT_w = 0.3 ºC. Then the computed temperature at the fourth section line is T_w = 10.1 ºC. By comparison, the observed water temperature was 10 ^{o}C. When computing temperature at the fourth section line at 20.00, water leaves the dam at hour 15.00 on July, 2. As it flows downstream its temperature changes by ΔT_w = 1.2 ºC when reaching the second station, by ΔT_w = 0.4 ºC reaching the third section line and by ΔT_w = 1.5 ºC when finally reaching the fourth section line. The predicted temperature at the fourth section line is T_w = 10.3 ºC. The observed temperature recorded at that station at 20.00 on July, 3 was T_w = 10.6 ºC.

Conclusion

We have proposed a simple model for simulating summertime hydrothermal regime of a river based on calculation of water temperature in a co-ordinate system moving with water. The physically based estimation of water heat budget takes into account absorption of solar radiation by water surface, emission and absorption of atmospheric TIR by water, convective heating of water as well as heat loss due to evaporative processes. The temporal fluctuation pattern of direct and scattered solar radiation depends on the zenith angle and atmospheric absorption. The dominant water heating factor is solar radiation during the daytime and atmospheric TIR at night. Water temperatures 124 km downstream of the Krasnoyarsk HPP on the Yenisei River computed using the proposed model with consideration of morphometric characteristics are close to the recorded temperatures observed at the gauging stations, which proves that the deployed physical-mathematical model provides an adequate description of the actual hydrothermal processes. Our spatial-temporal analysis has revealed no diurnal fluctuations of water temperature, which we attribute to the fact that *cold* water leaving the dam enters the *warm* surrounding environment providing a permanent source of water heating.

Acknowledgment

This work was carried out with partial financial support from the Russian Foundation for Basic Research and the Government of the Krasnoyarsk Territory (project No. 18-41-242006 p_mk)

The authors are greateful V.M. Belolipitskii and A.P. Gavriluk for the discussion of the results of work; D.A. Burakov for providing data on water temperatures recorder at river stations; O.E. Yakubailik for providing morphometric data.

References

[1] Dingman, S. L., *Physical Hydrology*, 3rd ed., Waveland Press. Inc. Long Grove, Ill., USA, 2015
[2] Sinokrot, B. A., Stefan, H. G., Stream Temperature Dynamics: Measurements and Modelling, *Water Resour. Res. 29* (1993), 7, pp. 2299-2312
[3] Mohseni, O., Stefan, H. G., Stream Temperature/Air Temperature Relationship: a Physical Interpretation, *J. Hydrol., 218* (1999), 3-4, pp. 128-141
[4] Lowney, C. L., Stream Temperature Variation in Regulated Rivers: Evidence for a Spatial Pattern in Daily Minimum and Maximum Magnitudes, *Water Resour. Res., 36* (2000), 10, pp. 2947-2955
[5] Yu, H., *et al*., Study on Temperature Distribution Due to Freezing and Thawing at the Fengman Concrete Gravity Dam, *Thermal Science, 15* (2011), Suppl. 1, pp. S27-S32
[6] Belolipetsii, V. M., *et al*., *Numerical Modeling of the Problems the Channel Way in hydro-Ice-Thermies* (in Russian), Novosibirsk, Russian Academy of Science, Siberian Division, Novosibirsk, Russia, 1993

[7] Iqbal, M., *An Introduction to Solar Radiation*, Academic Press Canadian: Library of Congress Cataloging in Publication Data, Wasington DC, 1983
[8] Handcock, R. N., *et al*, Thermal Infrared Remote Sensing of Water Temperature in Riverine Hands Capes, in: *Fluvial Remote Sensing for Science and Management*, 1st ed.. (Ed. P. E. Charbonneau, H. Piegay). John Wiley and Sons, Ltd, New York, USA, 2012
[9] Flerchinger, G. N., *et al*., Comparison of Algorithms for Incoming Atmospheric Long-Wave Radiation. *Water Resources Research, 45* (2009) 3, W03423
[10] Iziomon, M. G., *et al*., Downward Atmospheric Longwave Irradiance under Clear and Cloudy Skies: Measurement and Parametrization, *J. Atmosph. Solar Terrestrial Phys. 65* (2003), 10, pp. 1107-1116
[11] Rees, W. G., *Physical Principles of Remote Sensing*, 2nd ed., Cambridge University Press, Cambridge, Mass., USA, 2001
[12] Shulyakovskui, L. G, Formula for Computing Evaporation with Allowance for the Temperature of Free Water Surface, *Hydrol. Sel. Par., 6* (1969), pp. 566-573
[13] Ryan, P. J., Harleman, D. R. F., An Analytical and Experimental Study of transient Cooling Pond Behavior, Rep. No. 161, Parsons Laboratory for Water Resources and Hydrodynamics, Massacuse Institute of Technology, Cambridge, Mass., USA, 1973
[14] Gulliver, J. S., Stefan, H. G., Wind Function for Sheltered Stream, *J. Envir. Eng. 112* (1986), 2, pp. 1-14
[15] Boyd, M., Kasper, B., Analytical methods for Dynamic Open Channel Heat and Mass Transfer: methodology for heat Source Model Version 7.0, https://www.oregon.gov/deg/FilterDocs/heatsourcemanual.pdf
[16] Bowen. I. S., The Ration of Heat Losses by Conduction and by Evaporation from Any Water Surface, *Phys. Rew., 27* (1926), 6, pp. 749-787

Paper submitted: October 10, 2018
Paper revised: November 10, 2018
Paper accepted: November 22, 2018